PCCP

Low temperature FT-IR and molecular orbital study of *N*,*N*-dimethylglycine methyl ester: Proof for different ground conformational states in gas phase and in condensed media†

A. Gómez-Zavaglia[ab] and R. Fausto*[a]

[a] *Department of Chemistry, University of Coimbra, P-3004-535, Portugal*
[b] *Facultad de Farmacia y Bioquímica, Universidad de Buenos Aires, RA-1113, Argentina.*
E-mail: rfausto@ci.uc.pt

Received 23rd September 2002, Accepted 30th October 2002
First published as an Advance Article on the web 15th November 2002

N,*N*-dimethylglycine methyl ester (DMG-Me) was studied by FT-IR spectroscopy under several experimental conditions, including low temperature solid state and isolated in low temperature inert gas matrices, and by molecular orbital calculations. In agreement with the theoretical predictions, the experimental data show that in the gaseous phase the most stable conformer (ASC) has the ester group in *cis* configuration and the N–C–C=O and Lp–N–C–C (Lp = lone electron pair) dihedral angles equal to 0° and 180°, respectively, while the first conformational excited state corresponds to the doubly-degenerated-by-symmetry GSC form, where the Lp–N–C–C axis is *gauche*-oriented (±46.5°). On the other hand, for the matrix isolated molecule as well as in both the liquid and low temperature solid states the relative stability of the two lowest energy conformers of DMG-Me is reversed, the more polar GSC form becoming the ground conformational state. This molecule is then a remarkable example of a system showing an inversion in the order of its lowest energy conformational states due to a minor perturbation by the media such as that due to the inert gas matrix. Full assignment of the spectra obtained in the different experimental conditions used is also presented.

Introduction

N,*N*-dimethylglycine (DMG) is a product of the metabolic pathways of choline and aminoacids and is currently used as an anti-stress nutrient in diet tablets and "energetic drinks" for sportsmen.[1] Recently, DMG esters were proposed as new derivatives for the rapid, sensitive and selective analysis of primary and secondary alcohols in complex mixtures, by electronspray ionization tandem mass spectrometry (ESI-MS-MS).[2] These esters have also been used as first reagents in the synthesis of lipids, including choline.[3,4] The *N*,*N*-dimethylglycine methyl ester (DMG-Me) is the canonical analogue of the permanent zwitterionic species betaine (*N*,*N*,*N*-trimethylglycine), whose biochemical relevance is also well known.[5–7]

In a previous study, we have investigated DMG isolated in low temperature inert gas matrices by FT-IR spectroscopy.[8] The analysis of the experimental data was supported by extensive quantum chemical calculations undertaken at both DFT and MP2 levels of theory. In that study, the spectral signatures of the three lowest energy conformers of neutral monomeric DMG were characterized for the first time. The conformational ground state was found to be the intramolecularly O–H···N hydrogen-bonded GAT form, where the Lp–N–C–C and N–C–C=O dihedral angles are 30° and *ca.* 180°, respectively, and the carboxylic group assumes a *trans* configuration. In the second (ASC) and third (GSC) lowest energy forms of DMG, the carboxylic moiety assumes a *cis* conformation, while the N–C–C=O axis adopts the *syn* arrangement and the conformation around the N–C bond is, respectively, *anti* and *gauche*. The presence of the intramolecular hydrogen bond was found to be essential in the stabilization of the ground conformational state in DMG.[8] In DMG-Me, however, this interaction cannot operate due to the replacement of the acid hydrogen atom by the methyl ester group, and a significantly different conformational behavior can then be expected for this compound.

Taking into consideration the results for DMG, the ASC and GSC conformations (which correspond to the second and third most stable conformers in DMG[8]) could be expected to be the most stable structures of DMG-Me. However, in the unique structural study reported so far,[9] these conformations were neglected by the authors, since they were essentially interested to determine the electron binding energies of DMG-Me and the small dipole moments of both ASC and GSC are not large enough to allow the molecule to bind an excess electron. Instead, higher energy conformations with a *trans* carboxylic group and a larger dipole moment were considered.[9] Hence, in practical terms, DMG-Me had not yet been characterized structurally until now. Moreover, no vibrational data was reported so far.

Since the ASC and GSC conformers in DMG were found to have relatively similar energies ($\Delta E_{GSC\text{-}ASC} \approx 2$ kJ mol^{-1})[8] and we have been particularly interested in our laboratory to investigate the influence of media on the relative stability of nearly accidentally degenerated conformers,[10–12] DMG-Me appears, also from this perspective, as a potentially interesting and challenging molecular system to be studied. In this paper we report the results of an FT-IR spectroscopic study of DMG-Me in a variety of experimental conditions, which includes the liquid phase, the low temperature solid states and the matrix-isolated species in both argon and xenon matrices. These studies were complemented with molecular orbital calculations undertaken at the density functional theory (DFT) and second order Møller–Plesset (MP2) levels.

† Electronic supplementary information (ESI) available: calculated geometries and rotational constants for the most stable conformers of dimethylglycine methyl ester. See http://www.rsc.org/suppdata/cp/b2/b209311c/

 DOI: 10.1039/b209311c

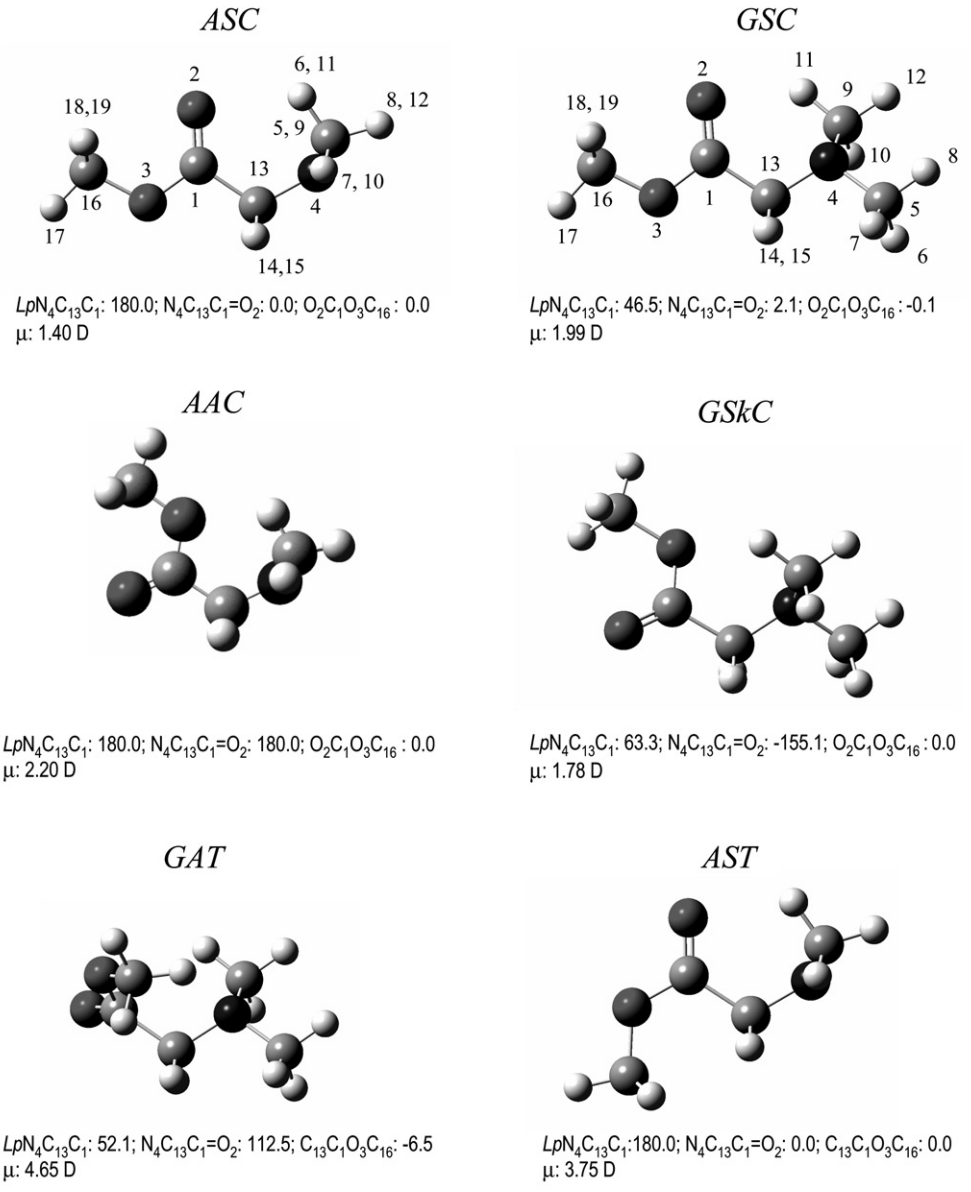

Fig. 1 Lowest energy conformers of neutral DMG-Me with atom numbering scheme. For convenience, the values of main dihedral angles (degrees) and dipole moments (Debye) are included.

Materials and methods

Computational methodology

The quantum chemical calculations were performed with Gaussian 98[13] at the DFT and MP2 levels of theory, using the 6-311++G** and 6-31++G** basis sets, respectively.[14] The DFT calculations were carried out with the three-parameter density functional abbreviated as B3LYP, which includes Becke's gradient exchange correction,[15] the Lee, Yang, Parr correlation functional[16] and the Vosko, Wilk and Nusair correlation functional.[17]

Conformations were optimized at each level of theory using the geometry direct inversion of the invariant subspace (GDIIS) method.[18] Vibrational frequencies were calculated at the DFT level and the nature of the critical points on the potential energy surface resulting from optimisation was determined by inspection of the corresponding calculated Hessian matrix. All optimised structures were confirmed to be minimum energy conformations. The calculated frequencies were scaled down by a single factor (0.978) to correct them for the effects of basis set limitations, neglected part of electron correlation and anharmonicity effects, and used to assist the analysis of the experimental spectra. Normal coordinates analyses were undertaken in the internal coordinates space as described by Schachtschneider[19] using the program BALGA and the optimised geometries and harmonic force constants resulting from

Table 1 Relative energies (ΔE_{ZPE}), including zero point vibrational contributions, for the various conformers of DMG-Me[a]

Conformer	DFT(B3LYP)/6-311++G** ΔE_{ZPE}	MP2/6-31++G** ΔE_{ZPE}[b]
ASC	0.0 (−1 056 252.97)[c]	0.0 (−1 052 887.44)[c]
GSC	2.72	3.17
AAC	4.93	4.48
GSkC	6.37	4.66
GAT	33.03	30.28
AST	34.20	36.94

[a] Energies in kJ mol^{-1}; conformers are depicted in Fig. 1. [b] Zero point energy corrections taken from DFT(B3LYP)/6-311++G** calculations. [c] Total energies with zero point vibrational energy contribution in parentheses.

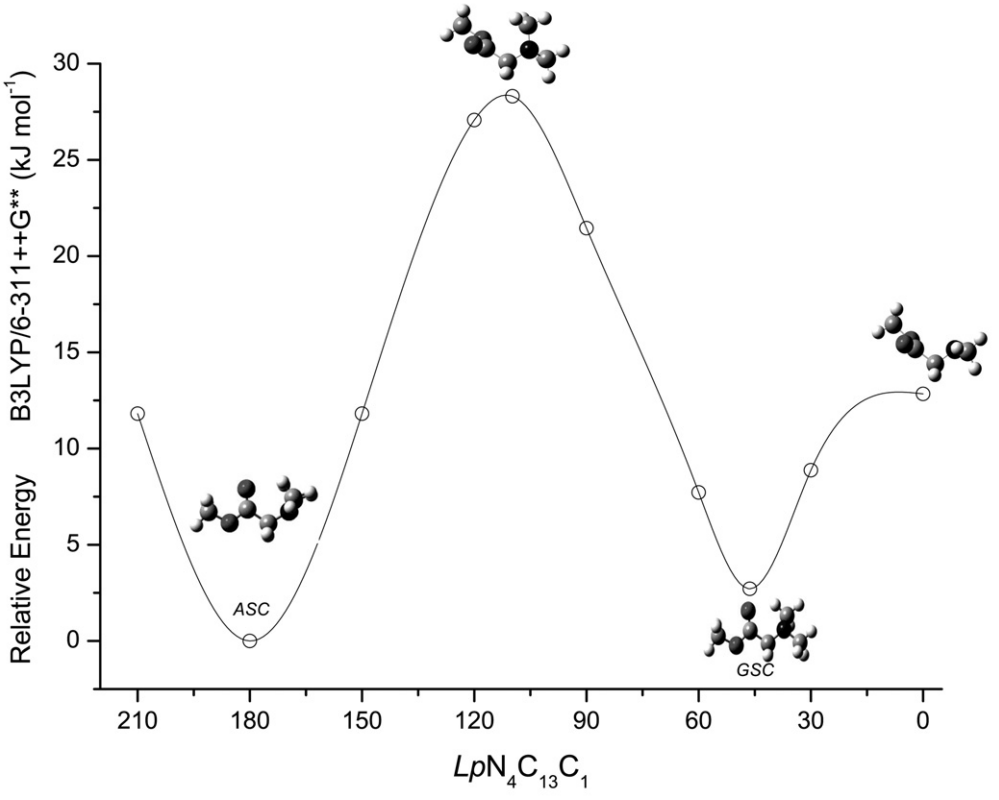

Fig. 2 DFT(B3LYP)/6-311++G** calculated potential energy profile for internal rotation around the N_4–C_{13} bond (ASC ↔ GSC ↔ GSC′ interconversion).

the DFT(B3LYP)/6-311++G** calculations. Potential energy profiles for internal rotation were calculated performing a relaxed scan on the potential energy surface (PES) along the reaction coordinate and the transition state structures for conformational interconversion obtained using the synchronous transit-guided quasi-newton (STQN) method.[20]

Infrared spectroscopy

N,*N*-dimethylglycine methyl ester was obtained spectroscopic grade from Tokyo Kasei Kogyo. The IR spectra were collected on a Mattson (Infinity 60AR Series) or Bomem (MB40) Fourier transform infrared spectrometer equipped with a deuterated triglycine sulfate (DTGS) detector and Ge/KBr and Zn/Se beamsplitters, respectively, with 0.5 cm^{-1} or 1 cm^{-1} (for liquid phase studies) spectral resolution.

In the matrix isolation experiments, a glass vacuum system and standard manometric procedures were used to deposit the matrix gas (argon, 99.99990%; xenon, 99.995%, obtained from Air Liquid). Matrices were prepared by co-deposition, onto the cooled CsI substrate of the cryostat, of the matrix gas and DMG-Me placed in a specially designed doubly termostattable Knudsen cell with shut-off possibility whose main component is a NUPRO SS-4BMRG needle valve. The temperature of the cell can be controlled separately in the valve nozzle and the sample compartment, enabling a more precise control of the saturated gas pressure over the liquid DMG-Me and a better metering function of the valve. Further details of the experimental setup can be found in ref. 21 All experiments were done on the basis of an APD Cryogenics close-cycle helium refrigeration system with a DE-202A expander. Deposition temperatures ranged from 9 to 20 K. Necessary modifications of the sample compartment of the spectrometer were made in order to accommodate the cryostat head and allow efficient purging of the instrument by a stream of dry air to remove water and CO_2 vapours. After depositing the compound, annealing experiments were performed until a temperature of 30 K and 60 K for Ar and Xe, respectively.

The low temperature solid amorphous layer was prepared in the same way as matrices but with the flux of matrix gas cut off. The layer was then allowed to anneal at slowly increasing temperature up to 154 K. IR spectra were collected during this process every 10 to 20 K of temperature change. After the temperature exceeded 154 K the substrate was cooled back to 9 K and spectra collected each 10–20 K once more. Two cycles of annealing were performed by heating and cooling the sample between 9 and 154 K.

For liquid state experiments a thin film of the compound was pressed within two sealed KBr windows assembled in a SPECAC variable temperature cell controlled by a Red Lions digital temperature controller.

Results and discussion

Molecular geometries and energies

A systematic search on the potential energy surface of DMG-Me both at the DFT(B3LYP)/6-311++G** and MP2/6-31++G** levels of theory enabled us to identify six different conformers (Fig. 1). The four lowest energy conformers exhibit a *cis* carboxylic ester group (O=C–O–C dihedral equal to 0°), while the remaining two conformers have this group in a *trans* configuration (O=C–O–C axis equal to 180°) and correspond to high energy forms with relative energies to the conformational ground state larger than 30 kJ mol^{-1}. The calculated relative energies of the various conformers are presented in Table 1, while the calculated geometries and rotational constants for the two most stable conformers (ASC and GSC; see Fig. 1) are given in the electronic supplementary material Table S1.†‡According to the theoretical predictions, the

‡ Calculated geometries and rotational constants for the higher energy conformers are available from the corresponding author upon request.

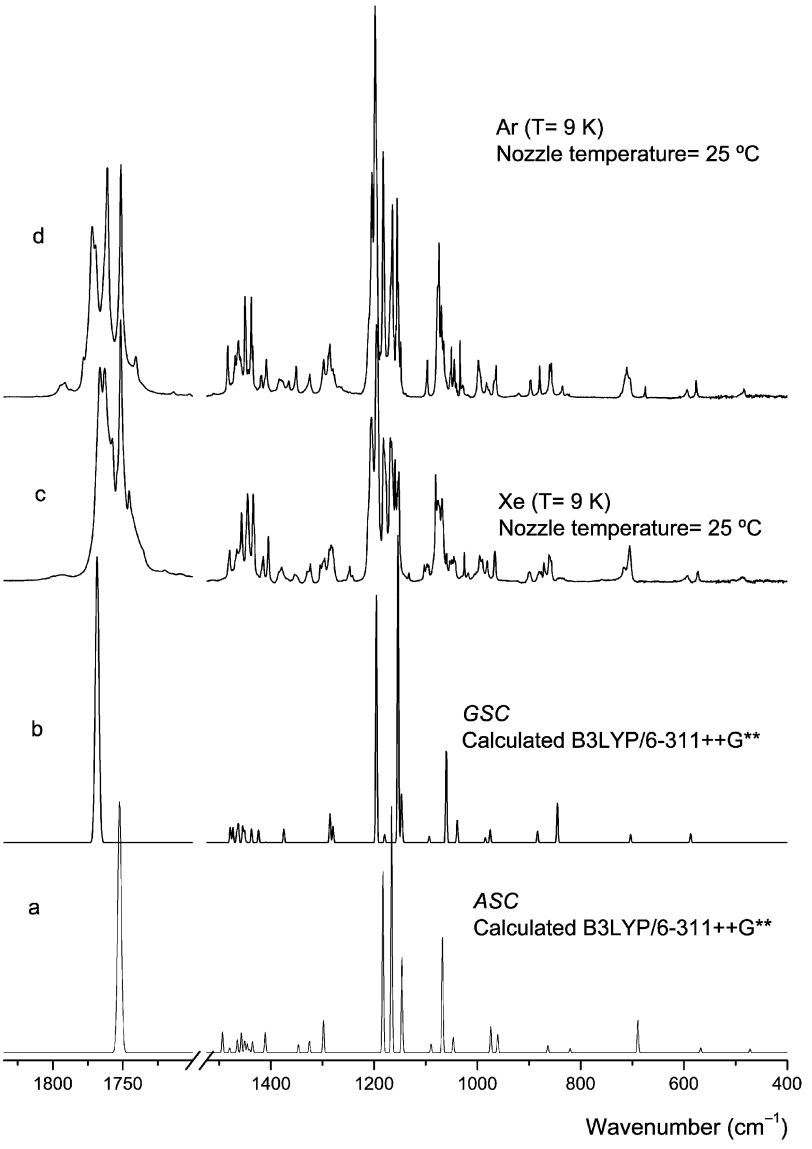

Fig. 3 Infrared spectra of DMG-Me trapped in argon and xenon matrices (spectra obtained immediately after deposition at 9 K) and calculated spectra for ASC and GSC conformers.

conformational ground state of DMG-Me corresponds to the ASC conformer, where the N–C–C=O and Lp–N–C–C (Lp = lone electron pair) dihedral angles are 0° and 180°, respectively. The second most stable conformer, GSC, is a doubly-degenerated-by-symmetry form, differing from the most stable conformer in the Lp–N–C–C axis, which assumes a *gauche* (±46.5°) configuration. These two conformers differ in energy only by *ca.* 3 kJ mol^{-1} and are similar to the second and third more stable conformers of the parent *N*,*N*-dimethylglycine molecule (as mentioned before, for that molecule the most stable conformer was found to be the intramolecularly O–H···N hydrogen-bonded GAT form[8] that has no equivalent form in DMG-Me since in this latter molecule the hydroxylic hydrogen atom has been replaced by the methyl ester group). The third conformer of DMG-Me (AAC; see Fig. 1) is a symmetric form with planar heavy atom backbone where both N–C–C=O and Lp–N–C–C assume the *anti* configuration (180°), while the fourth conformer (GSkC; see Fig. 1) is also a doubly-degenerated-by-symmetry form, with (N–C–C=O; Lp–N–C–C) dihedral angles of (−155.1°; 63.3°) or (155.1°; −63.3°). These forms are predicted to have relatively similar energies, within the range 4.5–6.5 kJ mol^{-1} relatively to the most stable form (see Table 1). Hence, assuming the Boltzman distribution, the two most stable conformers of the studied molecule are predicted by the calculations to account for about 75% of the population, at room temperature.

Fig. 2 shows the potential energy profile for interconversion between the two most stable conformers of DMG-Me and between the two equivalent-by-symmetry GSC conformers calculated at the DFT(B3LYP)/6-311++G** level of theory. To obtain this energy profile, the Lp–N–C–C dihedral angle was incremented by 30° and at each point all remaining geometrical parameters were optimized. The transition state structures were obtained using the synchronous transit-guided quasi-newton (STQN) method.[20] The energy barriers associated with the ASC → GSC and GSC → GSC′ conformational interconversions are predicted to be 28.3 kJ mol^{-1} and 12.8 kJ mol^{-1}, respectively, being similar to those previously found for the corresponding isomerization reactions in *N*,*N*-dimethylglycine (29.4 kJ mol^{-1} and 13.6 kJ mol^{-1}[18]).

It is interesting to note that in general the calculated geometries for the two most stable conformers of DMG-Me are very similar (see electronic supplementary material, Table S1†), indicating that in these conformers the main intramolecular interactions should not differ very much. The largest difference found in the geometrical parameters occurs for the C5–N4–C13, C9–N4–C13 and C1–C13–N4 angles, which are *ca.* 3° larger in the ASC conformer due to the closest proximity of the

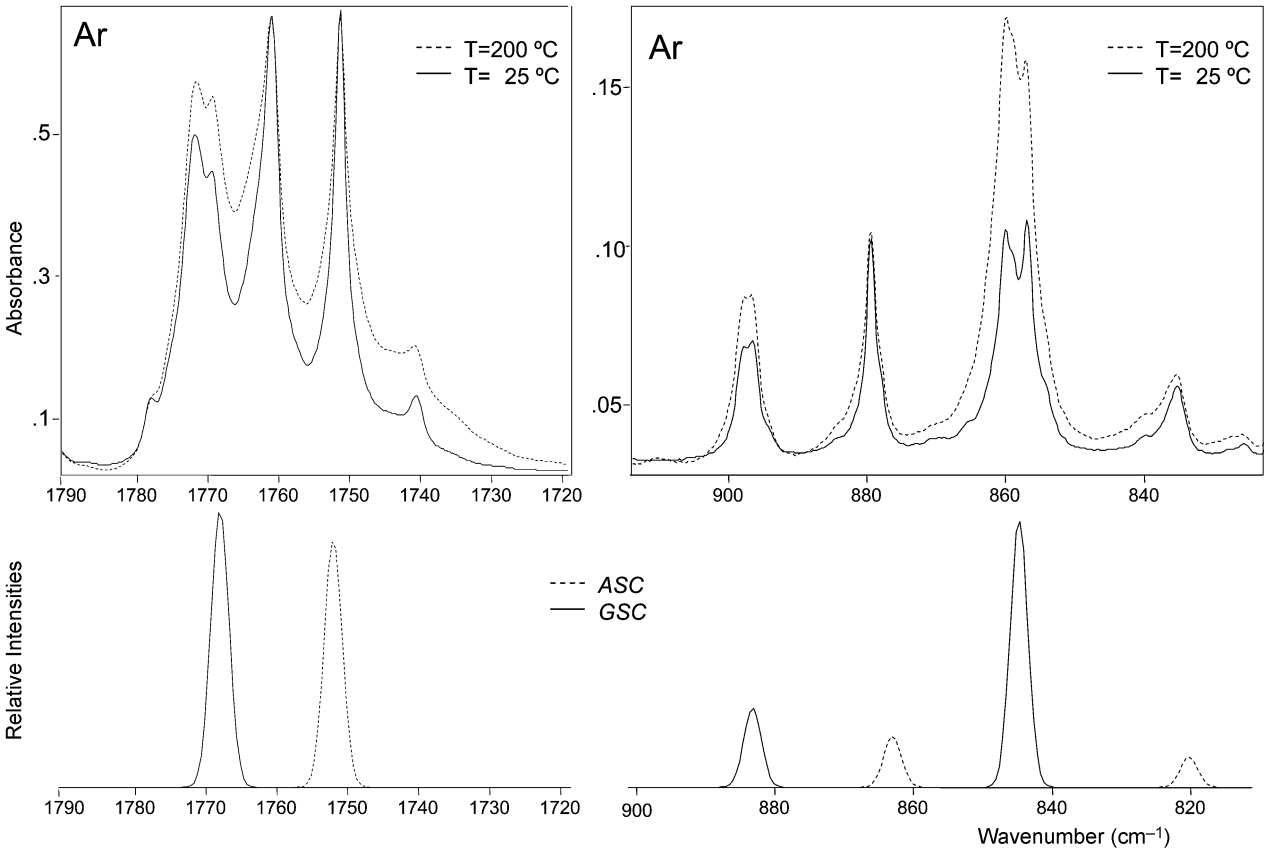

Fig. 4 Relevant spectral regions of the infrared spectrum of DMG-Me trapped in an argon matrix freshly prepared sample at 9 K (— nozzle temperature = 25 °C, and --- 200 °C), and calculated spectra for ASC and GSC conformers.

methyl groups from the carbonyl oxygen in this form. Indeed, the same conclusion could also be extracted by looking at the calculated Mülliken atomic charges in these two conformers (Table S2—electronic supplementary material†) that were also found to be quite similar except in the case of those of C1 and C13, which were predicted to be more positive and more negative, respectively, in the GSC conformer. These changes indicate a relatively higher charge separation in the GSC conformer, being in consonance with its larger dipole moment (1.99 D *vs.* 1.40 D in ASC; see Fig. 1). The N4–C13–H14 angle is also considerably different in ASC and GSC, being *ca.* 4° larger in the GSC conformer due to the repulsion between H14 and the closest methyl hydrogen atom H10 in this form.

Infrared spectra

The spectroscopic results are synthesised in Figs. 3–8 and Tables 2 and 3. The definition of the symmetry coordinates selected to perform the normal mode analysis and the potential energy distribution results for the relevant conformers of DMG-Me obtained from those calculations are presented in Tables S3–S5 (electronic supplementary material).†

Infrared spectra of DMG-Me in both argon and xenon matrices obtained by co-deposition of the vapour of the compound and the matrix-gas were obtained as described in the Experimental section. Different temperatures of the valve nozzle and of the cold substrate of the cryostat were used. From the whole set of experiments on the matrix-isolated compound the following main conclusions could be extracted:

(i) Two different conformers of DMG-Me contribute to the observed spectra in both argon and xenon matrices. Comparison of the experimental data with the theoretically predicted spectra (Fig. 3) revealed that the two conformers observed experimentally are the ASC and GSC forms, *i.e.*, the two lowest energy forms predicted by the calculations. Full assignment of the observed matrix spectra is presented in Table 2. In general, the calculated (scaled) spectra fit nicely the experimental data. The assignments to individual conformers were facilitated by the temperature dependence exhibited by the intensity of the bands, both upon annealing and changing the temperature of the vapour prior to deposition.

(ii) In consonance with the theoretical predictions, in the gaseous phase the ASC conformer was found to be the ground conformational state. Indeed, increasing the temperature of the valve nozzle led to increasing the relative population of the less stable GSC conformer. This is clearly illustrated in Fig. 4 which compares the spectra obtained for DMG-Me in argon using two different valve nozzle temperatures (25 and 200 °C). The spectral regions shown correspond to those where the νC=O, νC–C and νN–C sym stretching modes are predicted to occur in both conformers; the figure also shows the calculated spectra for the two forms, for comparison. Note that the observed features exhibit site splitting. Matrix site splitting was found to be more pronounced in argon than in xenon (see Table 2). This result may indicate that in argon the solute molecules are not allowed to relax so efficiently as in xenon in order to adjust themselves as best as possible to fit the matrix packing requirements.

The band at *ca.* 1740 cm^{-1} in the νC=O stretching region (Fig. 4) deserves a further comment. This band increases in intensity with the nozzle temperature. Since both AAC and GSkC conformers (the third and fourth more stable conformers of DMG-Me) are predicted to give rise to a νC=O band at a lower frequency than both ASC and GSC forms, this band could then be assigned to these conformers. However, there is no further experimental evidence of the presence of either AAC or GSkC in the matrices and the assignment of this band to the first overtone of the νC–C stretching vibration of the

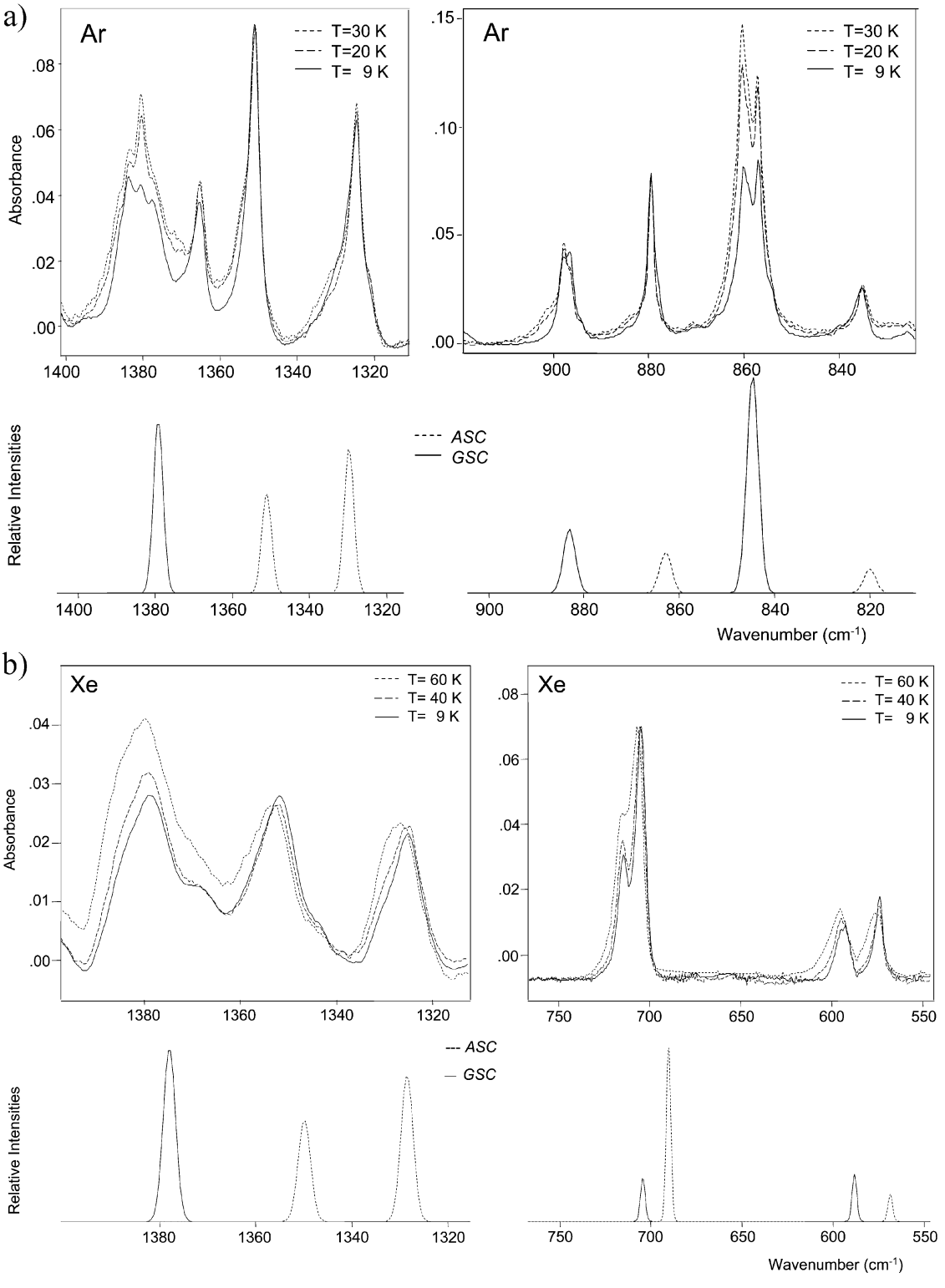

Fig. 5 Relevant spectral regions of the infrared spectrum of DMG-Me trapped in: (a) an argon matrix (— freshly prepared sample at 9 K; –·– after annealing at 20 K; and --- 30 K); (b) a Xenon matrix (— freshly prepared sample at 9 K; –·– after annealing at 40 K; and --- 60 K) and calculated spectra for ASC and GSC conformers. The pair of bands of the ASC conformer at 1351 and 1365 cm^{-1}, observed in argon, is ascribable to the ωCH_2 mode involved in a Fermi resonance interaction with the first overtone of the δOCO bending mode (whose fundamental is observed in the 710–705 cm^{-1}; see Table 2).

GSC form, whose fundamental appears at *ca.* 895 cm^{-1} (Table 2), seems to be more plausible.

(iii) Annealing of the matrices (both argon and xenon) led to partial conversion of the ASC conformer into the GSC form (Fig. 5). This result indicates that in the matrices the order of stability of the two conformers changes relatively to the gaseous phase, the GSC conformer becoming the ground conformational state. The GSC conformer has a larger dipole moment than the ASC form (1.99 *vs.* 1.40 D; see Fig. 1) and thus it could be expected to be stabilized in the matrices with regard to the gaseous phase. Nevertheless, this molecule is a remarkable example of a system showing an inversion in the order of its lowest energy conformational states due to a relatively minor perturbation by the media, such as that due to the inert gas matrix.

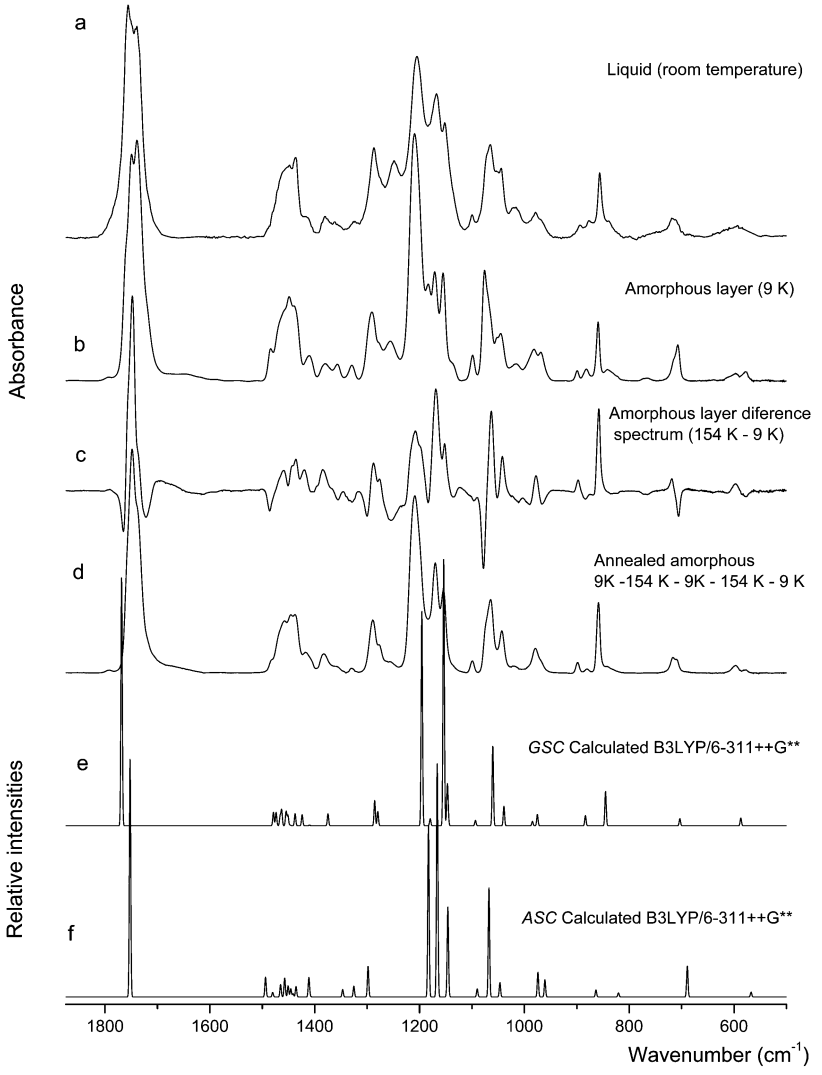

Fig. 6 Infrared spectra of DMG-Me (a) in the liquid state (room temperature); (b) solid amorphous layer at 9 K; (c) amorphous layer difference spectrum (154 K–9 K); (d) annealed amorphous sample. (e) and (f) Calculated spectra for GSC and ASC monomers, respectively.

(iv) The relative populations of the ASC and GSC conformers observed in argon and xenon matrices prepared using the same experimental conditions (valve nozzle and substrate temperatures; concentration; matrix-gas flux) were found to differ considerably, with the GSC form showing a larger relative population in xenon than in argon (see Fig. 3). This is in consonance with the known better trapping ability of argon when compared with xenon or, in other words, with the generally greater conformational cooling effects observable when xenon is used as the matrix gas.[12,22] Note that in the present case, the consequences of a more important conformational cooling effect in xenon are different from the usually observed phenomena when the conformational ground state is the same in both the gaseous phase and in the matrices. In the trivial situation, the most abundant conformer in the gas phase has its relative population further increased in the xenon matrix due to the conformational cooling; in DMG-Me, due to the inversion of the relative stability of the two conformational states, the most abundant conformer in the gaseous phase has its relative population decreased in the xenon matrix due to the conformational cooling.

The spectrum of the low temperature amorphous layer obtained by deposition of the vapour of the compound onto the cold substrate of the cryostat (at 9 K) does also reveal the presence of both ASC and GSC conformers. This spectrum is compared with the calculated spectra for the two forms in Fig. 6. Assignments are presented in Table 3. Fig. 6 also shows the difference spectrum obtained by subtracting from the spectrum of the annealed ($T = 154$ K) amorphous layer the spectrum of the freshly prepared amorphous ($T = 9$ K) layer. In the difference spectrum, the bands pointing upwards are due to the GSC conformer, while those pointing to the bottom belong to the ASC form. Hence, annealing the amorphous layer to higher temperatures leads to increase the population of the GSC conformer relatively to ASC. Upon reaching 154 K, the sample was cooled again to 9 K without observation of any substantial change in the spectrum. However, the subsequent rewarming of the sample further increases the relative population of the GSC conformer, in such a way that the bands due to ASC practically vanish (see spectrum d, in Fig. 6). These results can be interpreted as follows: upon deposition of the vapour into the cold substrate, the conformers present in the gaseous phase are frozen, contributing to the spectrum of the freshly prepared amorphous layer; annealing of the sample enables the molecules of the compound to relax and attain the conformation that is most stable under these conditions, which corresponds to the most polar GSC conformer; on cooling, no changes occur, but, when subjected to a new warming cycle, the sample can further relax and attain a quasi-crystalline state, where almost all molecules assume the GSC conformation.

In the liquid state spectra at room temperature (spectrum a, in Fig. 6), features due to the two conformers can also be

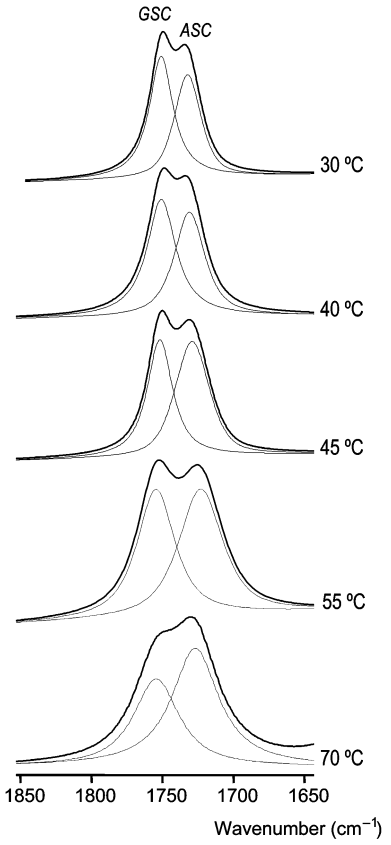

Fig. 7 Temperature dependence of the νC=O region for DMG-Me in the liquid state showing results of band deconvolution. Besides the change in the relative band intensities, note that the expected increase in the bandwidths with temperature is quite clear.

clearly identified. Indeed, the spectrum of the liquid closely resembles that of the amorphous state (trace b, in Fig. 6). It is, however, easily noticed that the population of the GSC conformer is higher in the room temperature liquid than in the freshly prepared amorphous layer. For example, the carbonyl stretching band appears as a doublet in both spectra, with the higher frequency component, ascribable to the GSC form, being more intense than the lower component band in the spectrum of the liquid, while the opposite situation occurs in the spectrum of the amorphous layer. Since the amorphous results from the frozen vapour of the compound and in the

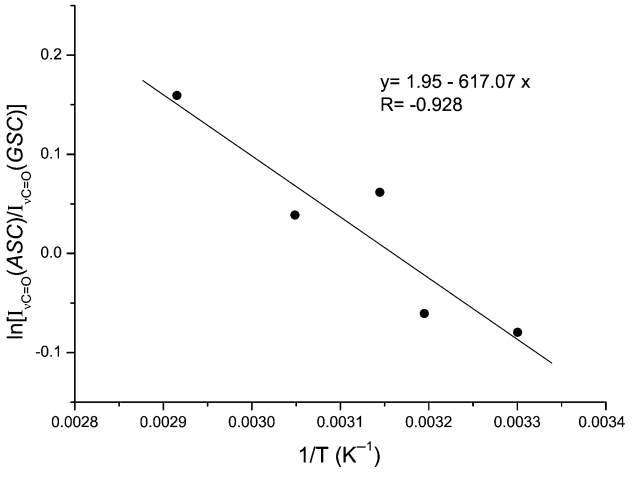

Fig. 8 Van't Hoff plot of ln $[I_{\nu C=O}(ASC)/I_{\nu C=O}(GSC)]$ *vs* $1/T$ (K^{-1}) for DMG-Me.

gaseous phase ASC is the most stable form, whereas in the liquid phase the more polar GSC form is the minimum energy conformer, the observed data can be easily understood.

The temperature dependence of the carbonyl stretching bands is presented in Fig. 7. Since the ASC form is the higher energy conformer of DMG-Me in the liquid, its relative population must increase relatively to that of the GSC conformer upon increasing the temperature. Accordingly, the intensity of the band appearing at *ca.* 1740 cm^{-1}, ascribed to ASC increases with temperature relatively to that due to the same mode in the GSC form, which is observed at *ca.* 1750 cm^{-1}. The integrated intensities of the νC=O bands due to each conformer were obtained after being subjected to deconvolution (see Fig. 7) and from these a Van't Hoff plot of $\ln(I_{ASC}/I_{GSC})$ *vs.* the reciprocal temperature was obtained (Fig. 8), yielding an enthalpy difference between the conformers in the liquid phase of 5.13 kJ mol^{-1}, favouring the GSC form This value may be compared with the theoretical value obtained for the gas: *ca.* 3 kJ mol^{-1}, favouring the ASC form. Hence, a stabilization of *ca.* 8 kJ mol^{-1} of the more polar GSC conformer relative to the ASC form occurs upon going from the gas phase to the liquid state due to intermolecular interactions (dipolar interactions are certainly the prevalent effects). With all probability, a similar stabilization of the GSC form relative to the ASC conformer should also occur in the case of the amorphous solid state.

Conclusion

In agreement with the theoretical predictions, FT-IR spectroscopic studies on DMG-Me isolated in both argon and xenon matrices enabled to conclude that in the gaseous phase the most stable conformer of the studied compound is the ASC conformer, which exhibits the ester group in *cis* configuration and the N–C–C=O and Lp–N–C–C (Lp = lone electron pair) dihedral angles equal to 0° and 180°, respectively, while the first conformational excited state corresponds to the doubly-degenerated-by-symmetry GSC form, where the Lp–N–C–C axis is *gauche* (±46.5°). On the other hand, for the matrix isolated molecule as well as in both the liquid and low temperature solid states the relative stability of the two lowest energy conformers of DMG-Me is reversed, the more polar GSC form becoming the ground conformational state. Indeed, DMG-Me appears as a remarkable example of a molecule showing an inversion in the order of its lowest energy conformational states due to a minor perturbation by the media such as that due to the inert gas matrix. In the liquid phase, GSC is more stable than ASC by *ca.* 5 kJ mol^{-1}, implying a stabilization of *ca.* 8 kJ mol^{-1} in going from the gas phase to the liquid state of the first conformer relative to the second one.

Taking into consideration the theoretically predicted spectra for the two experimentally observed conformers and the different experiments undertaken (*e.g.*, temperature variation studies in different conditions; change of matrix gas, valve nozzle and of deposition temperatures) full assignment of the spectra obtained for the compound in the various phases studies could be made successfully.

Acknowledgements

The authors thank Dr I. D. Reva for his helpful comments on this paper and technical help. Technical support from Dr J. O. Cecílio is also acknowledged. This work was supported by the Portuguese Fundação para a Ciência e a Tecnologia (Research Project POCTI/QUI/43366/2001 and Grant FCT #SFRH/BPD/1661/2000). A. G.-Z. acknowledges the post-doctoral grant from the Instituto para a Cooperação Científica e Tecnológica Internacional (ICCTI), Lisbon.

Table 2 Calculated [scaled, DFT (B3LYP)/6-311++G**] frequencies for conformers ASC and GSC of DMG-Me and observed frequencies for the compound in xenon and argon matrixes at 9 K [a]

				Observed frequency	
Approximate description	Conformer	Calculated frequency	Calculated intensity	Argon	Xenon
$\nu OCH_3as'$	ASC	3087.0	14.7	3036.7	3021.6
	GSC	3053.4	19.8	3007.0	3021.6
$\nu OCH_3as''$	ASC	3053.9	19.9	3007.0	3021.6
	GSC	3086.2	14.1	3036.7	3021.6
$\nu CH_3as''(2)$	ASC	3017.7	54.4	2978.7	2974.0
	GSC	3062.4	9.4	3007.0	2988.7
$\nu CH_3as''(1)$	ASC	3015.2	15.9	2974.9	2988.7
	GSC	3030.7	31.2	2983.0	2988.7
νCH_2as	ASC	2994.3	8.9	2963.0	2964.0
	GSC	2997.9	12.7	2963.0	2964.0
νOCH_3s	ASC	2983.2	20.4	2946.8	2946.5
	GSC	2982.8	35.0	2946.8	2946.5
$\nu CH_3as'(2)$	ASC	2982.5	33.8	2946.8	2946.5
	GSC	2988.0	29.8	2963.0	2964.0
$\nu CH_3as'(1)$	ASC	2982.0	53.2	2946.8/2948.1	2946.5
	GSC	2848.4	190.0	2850.6/2835.3/2823.4	2816.1/2843.7/2828.9
νCH_2s	ASC	2959.5	21.5	2913.5	2934.4
	GSC	2832.4	46.8	2778.6	2770.7
$\nu CH_3s(1)$	ASC	2913.0	69.7	2899.6/2888.7	2890.5/2881.6
	GSC	3006.0	27.2	2967.8	2974.0
$\nu CH_3s(2)$	ASC	2906.5	66.5	2875.5	2866.8
	GSC	2836.9	47.8	2799.6/2794.8	2793.1
$\nu C{=}O$	ASC	1752.3	208.2	1761.0/1751.3	1757.2/1754.0/1751.4
	GSC	1768.4	232.5	1778.0/1771.9/1769.5	1766.0/1763.1/1759.6
$\delta CH_3as''(1)$	ASC	1493.8	17.3	1483.4	1480.0
	GSC	1478.7	12.5	1471.9	Non obs.
$\delta CH_3as''(2)$	ASC	1480.1	3.9	1476.0	Non obs.
	GSC	1463.0	14.7	1462.8	1462.1
$\delta OCH_3as'$	ASC	1465.1	10.8	1465.1	1462.1
	GSC	1451.1	9.8	1449.0	1445.2
$\delta CH_3as'(1)$	ASC	1457.3	16.6	1459.4	1456.7
	GSC	1473.6	12.4	1469.2	1465.7
$\delta OCH_3as''$	ASC	1450.8	9.7	1449.0	1445.2
	GSC	1465.4	8.9	1462.8	1462.1
$\delta CH_3as'(2)$	ASC	1445.8	7.2	1458.3	Non obs.
	GSC	1454.5	13.4	1450.0	1445.2
$\delta CH_3s(1)$	ASC	1441.4	2.8	1443.9	Non obs.
	GSC	1447.2	0.7	Non obs.	Non obs.
δOCH_3s	ASC	1435.7	9.1	1435.1	1432.2
	GSC	1437.5	11.3	1437.8	1434.5
δCH_2	ASC	1411.2	16.7	1408.7	1404.2
	GSC	1424.0	10.2	1419.8/1418.1	1414.1
$\delta CH_3(2)$	ASC	1409.3	1.0	Non obs.	Non obs.
	GSC	1409.9	0.6	Non obs.	Non obs.
ωCH_2	ASC	1346.7	6.5	1351.0/1365.5	1352.4
	GSC	1374.8	11.2	1383.7/1380.6/1377.6	1383.7/1378.8
$twCH_2$	ASC	1325.3	9.5	1324.5	1324.7
	GSC	1285.6	23.6	1288.0/1285.8	1280
$\gamma CH_3'(1)$	ASC	1298.3	26.9	1297.8	1297.3
	GSC	1279.6	13.3	1279.8/1277.1	1278.7
$\gamma OCH_3'$	ASC	1182.9	149.0	1198.2/1195.2	1194.7
	GSC	1145.5	7.2	1157.7	1153.0
$\nu C{-}O$	ASC	1166.3	189.4	1182.5	1179.6
	GSC	1153.8	250.1	1168.5/1164.6/1161.5	1166.8
$\nu N{-}Cas$	ASC	1165.5	19.7	1182.5	1179.6
	GSC	1195.6	201.1	1210.2/1204.1	1204.8
$\gamma CH_3''(1)$	ASC	1146.1	77.6	1155.6	1153.0
	GSC	1147.0	35.8	1153.4	1155.6
$\gamma OCH_3''$	ASC	1144.5	1.5	1148.5	1152.2
	GSC	1179.7	6.6	1188.8	Non obs.
$\gamma CH_3''(2)$	ASC	1089.7	7.0	1096.9	1095.0
	GSC	1093.3	5.1	1098.3	1098.7
$\nu C{-}N$	ASC	1067.7	95.4	1076.6/1074.3	1076.7
	GSC	1060.3	74.9	1069.9/1065.5	1068.8
$\gamma CH_3'(2)$	ASC	1046.7	12.5	1052.5/1050.3	1051.6
	GSC	1039.1	18.2	1046.7/1044.9	1044.5

Table 2 (continued)

Approximate description	Conformer	Calculated frequency	Calculated intensity	Observed frequency	
				Argon	Xenon
νO–C	ASC	974.2	21.6	998.3/995.6/994.3	991.9
	GSC	984.7	4.0	1002.1	999.8
γCH_2	ASC	960.8	15.1	967.3/965.5/963.8	966.9
	GSC	975.3	10.7	982.4/980.3/977.4	980.7
νCC	ASC	863.4	6.0	879.4	879.7
	GSC	883.6	9.4	897.9/895.5	897.8
νN–Cs	ASC	820.6	3.6	839.7/835.2	836.8
	GSC	845.1	32.0	860.0/856.9	859.8
δOCO	ASC	689.2	27.0	710.5/705.2	704.9
	GSC	703.3	6.7	713.1	714.8
γC=O	ASC	567.6	4.2	576.4	573.9
	GSC	587.1	7.2	593.8	594.5
δCC=O	ASC	471.9	3.2	483.9	486.1
$\delta N(CH_3)_2$	GSC	475.4	0.2	483.9	486.1

[a] Frequencies in cm^{-1}; ν, bond stretching, δ, bending, γ rocking, ω wagging, tw, twisting, τ torsion. See Supplementary material (Tables S3–S5) for definition of symmetry coordinates, full set of calculated frequencies and intensities and PED.

Table 3 Calculated [scaled, DFT (B3LYP)/6-311++G**] frequencies for conformers ASC and GSC of DMG-Me and observed frequencies for the compound in the amorphous and annealed amorphous solid and liquid phase[a]

Approximate description	Conformer	Calculated frequency	Observed frequency		
			Amorphous (T = 9 K)	Annealed amorphous[b]	Liquid (room temperature)
νOCH_3as′	ASC	3087.0	3021.7		3026.7
	GSC	3053.4	2990.5	2998.7	2979.2
νOCH_3as″	ASC	3053.9	2990.5		2979.2
	GSC	3086.2	3021.7	3024.6/3019.9	3026.7
νCH_3as″(2)	ASC	3017.7	2968.8		2953.6
	GSC	3062.4	2990.5	3009.0/3003.4	2979.2
νCH_3as″(1)	ASC	3015.2	2968.8		2953.6
	GSC	3030.7	2990.5	2986.6	2979.2
νCH_2as	ASC	2994.3	Non obs.		Non obs.
	GSC	2997.9	Non obs.	Non obs.	Non obs.
νOCH_3s	ASC	2983.2	2936.0		2936.9
	GSC	2982.8	2953.7	2954.1	2953.6
νCH_3as′(2)	ASC	2982.5	2936.0		2936.9
	GSC	2988.0	2953.7	2960.6	2953.6
νCH_3as′(1)	ASC	2982.0	2936.0		2936.9
	GSC	2848.4	2822.6/2794.7	2852.5/2845.2/2832.2/2819.7/2800.2	2826.8/2795.1
νCH_2s	ASC	2959.5	2913.5		2906.1
	GSC	2832.4	2739.6	2745.8/2731.5	2737.9
νCH_3s(1)	ASC	2913.0	2871		2872.6
	GSC	3006.0	2953.7	2967.5	2953.6
νCH_3s(2)	ASC	2906.5	2871		2872.6
	GSC	2836.9	2773.9	2774.3/2767.8	2774.9
νC=O	ASC	1752.3	1739.8	1739.6	1739.3
	GSC	1768.4	1757.8/1749.2	1753.8/1746.6	1756.0/1749.9
δCH_3as″(1)	ASC	1493.8	1483.9		1480.9
	GSC	1478.7	Non obs.	1477.4	1475.4
δCH_3as″(2)	ASC	1480.1	Non obs.		Non obs.
	GSC	1463.0	1468.5	1463.3	1472.2
δOCH_3as′	ASC	1465.1	Non obs.		1472.2
	GSC	1451.1	1437.5	1436.7/1435.3	1436.1
δCH_3as′(1)	ASC	1457.3	1448.8	1451.3/1448.0	1448.0
	GSC	1473.6	1467.9	1471.8	1472.2
δOCH_3as″	ASC	1450.8	Non obs.		1456.8
	GSC	1465.4	1458.5	1463.3	1456.8
δCH_3as′(2)	ASC	1445.8	1429.3		1436.1
	GSC	1454.5	1442.7	1443.7/1441.2	1436.1
δCH_3s(1)	ASC	1441.4	1429.3		Non obs.
	GSC	1447.2	Non obs.	Non obs.	Non obs.
δOCH_3s	ASC	1435.7	1409.9		1413.1
	GSC	1437.5	1417.3	1423.0	1416.3

Table 3 (continued)

Approximate description	Conformer	Calculated frequency	Observed frequency		
			Amorphous (T = 9 K)	Annealed amorphous[b]	Liquid (room temperature)
δCH_2	ASC	1411.2	1409.9		1413.1
	GSC	1424.0	1417.3	1412.0	1416.3
$\delta CH_3(2)$	ASC	1409.3	Non obs.		1405.0
	GSC	1409.9	Non obs.	1406.4	1405.0
ωCH_2	ASC	1346.7	1356.8		1361.4
	GSC	1374.8	1379.6	1390.9/1385.3/1379.6	1380.2
$twCH_2$	ASC	1325.3	1329.1		1326.3
	GSC	1285.6	1288.7	1287.8/1283.8	1286.8
$\gamma CH_3'(1)$	ASC	1298.3	1299.2		1286.8
	GSC	1279.6	1277.3	1276.4	1276.0
$\gamma OCH_3'$	ASC	1182.9	1201.9		1204.7
	GSC	1145.5	Non obs.	Non obs.	Non obs.
$\nu C–O$	ASC	1166.3	1183.4		1180.5
	GSC	1153.8	1171.1	1172.9/1171.1/1163.6	1167.6
$\nu N–Cas$	ASC	1165.5	1183.4		1183.5
	GSC	1195.6	1209.4	1209.4/1204.1	1204.7
$\gamma CH_3''(1)$	ASC	1146.1	1137.0		1137.1
	GSC	1147.0	1155.0	1154.5	1151.7
$\gamma OCH_3''$	ASC	1144.5	Non obs.		Non obs.
	GSC	1179.7	Non obs.	1187.4	Non obs.
$\gamma CH_3''(2)$	ASC	1089.7	1097.1	1095.9	1099.6
	GSC	1093.3	1101.2	1104.7/1103.4/1099.1	1103.7
$\nu C–N$	ASC	1067.7	1075.9	1075.9	1072.0
	GSC	1060.3	1060.5	1071.4/1063.3	1064.9
$\gamma CH_3'(2)$	ASC	1046.7	1051.2		1052.4
	GSC	1039.1	1045.1	1048.3/1042.9/1037.3	1044.1
$\nu O–C$	ASC	974.2	989.2		990.2
	GSC	984.7	1015.7	1007.1	1015.9
γCH_2	ASC	960.8	968.5		970.2
	GSC	975.3	981.6	981.4/980.1/973.9	978.6
νCC	ASC	863.4	881.62		876.8
	GSC	883.6	899.2	900.4	894.0
$\nu N–Cs$	ASC	820.6	841.4		839.6
	GSC	845.1	859.2	871.3/861.2/857.3	856.3
δOCO	ASC	689.2	707.3		715.8
	GSC	703.3	717.0	724.3/777.0	738.0
$\gamma C=O$	ASC	567.6	578.2		594.9/594.5
	GSC	587.1	597.6	606.5/597.6	594.9/594.5
$\delta CC=O$	ASC	471.9	486.1		Not studied
$\delta N(CH_3)_2$	GSC	475.4	486.1	486.1	Not studied

[a] Frequencies in cm^{-1}; ν, bond stretching, δ, bending, γ rocking, ω wagging, tw, twisting, τ torsion. See Supplementary material (Tables S3–S5) for definition of symmetry coordinates, full set of calculated frequencies and intensities and PED. [b] Annealing was carried out by performing three heating/cooling cycles in between 9 and 154 K.

References

1 V. Rodrigues, J. Paixão, M. Costa and A. Matos Beja, *Acta Crystallogr., Sect. C: Cryst. Struct. Commun.*, 2001, **57**, 417.
2 D. W. Johnson, *J Mass Spectrom.*, 2001, **36**, 277.
3 S. Lin, R. I. Duclos Jr. and A. Makriyannis, *Chem. Phys. Lipids*, 1997, **86**, 171.
4 A. M. Aberle, F. Tablin, J. Zhu, N. J. Walker, D. C. Gruenert and M. H. Nantz, *Biochemistry*, 1998, **37**, 6533.
5 N. von Weymarn, A. Nyyssölä, T. Reinikainen, M. Leisola and H. Ojamo, *Appl. Microbiol. Biotechnol.*, 2001, **55**, 214.
6 M. L. Mendum and L. T. Smith, *Appl. Environ. Microbiol.*, 2002, **68**, 813.
7 T. van Der Heide and B. Poolman, *J. Bacteriol.*, 2000, **182**, 203.
8 A. Gómez-Zavaglia, I. D. Reva and R. Fausto, *Phys. Chem. Chem. Phys.* (DOI: 10.1039/b207320j).
9 J. Rak, P. Skurski and M. Gutowski, *J. Chem. Phys.*, 2001, **114**, 10 673.
10 I. D. Reva, S. V. Ilieva and R. Fausto, *Phys. Chem. Chem. Phys.*, 2001, **3**, 4235.
11 S. Lopes, L. Lapinski and R. Fausto, *Phys. Chem. Chem. Phys.* (DOI: 10.1039/b206270b).
12 I. D. Reva, S. G. Stepanian, L. Adamowicz and R. Fausto, *Phys. Chem. Chem. Phys.* (DOI: 10.1039/b210355a).
13 M. Frisch, G. Trucks, H. Schlegel, G. Scuseria, M. Robb, J. Cheeseman, V. Zakrzewski, J. Montgomery, R. Stratmann, K. Burant, S. Dapprich, J. Millam, A. Daniels, K. Kudin, M. Strain, O. Farkas, J. Tomasi, V. Barone, M. Cossi, R. Cammi, B. Mennucci, C. Pomelli, C. Adamo, S. Clifford, J. Ochterski, G. Petersson, P. Ayala, Q. Cui, K. Morokuma, D. Malick, A. Rabuck, K. Raghavachari, J. Foresman, J. Cioslowski, J. Ortiz, A. Baboul, B. Stefanov, G. Liu, A. Liashenko, P. Piskorz, I. Komaromi, R. Gomperts, R. Martin, D. Fox, T. Keith, M. Al-Laham, C. Peng, A. Nanayakkara, M. Challacombe, P. Gill, B. Johnson, W. Chen, M. Wong, J. Andres, C. Gonzalez, M. Head-Gordon, S. Replogle and J. Pople, 1998, Gaussian 98, revision A.9, Gaussian Inc., Pittsburgh, PA.
14 M. J. Frisch, M. Head-Gordon and J. A. Pople, *Chem. Phys. Lett.*, 1990, **166**, 281.
15 A. D. Becke, *Phys. Rev. Sect. A*, 1988, **38**, 3098.

16 C. T. Lee, W. T. Yang and R. G. Parr, *Phys. Rev. Sect. B*, 1988, **37**, 785.
17 S. H. Vosko, L. Wilk and M. Nusair, *Can. J. Phys*, 1980, **58**, 1200.
18 P. Csaszar and P. Pulay, *J. Mol. Struct. (THEOCHEM)*, 1984, **114**, 31.
19 J. H. Schachtschneider, Technical Report, Shell Development Co., Emeryville, CA, 1969.
20 C. Peng and H. B. Schlegel, *Isr. J. Chem.*, 1994, **33**, 449.
21 I. D. Reva, S. Stepanian, L. Adamowicz and R. Fausto, *J. Phys. Chem. A*, 2001, **105**, 4773.
22 R. S. Ruoff, T. D. Klots, T. Emilsson and H. S. Gutowsky, *J. Chem. Phys.*, 1990, **93**, 3142.